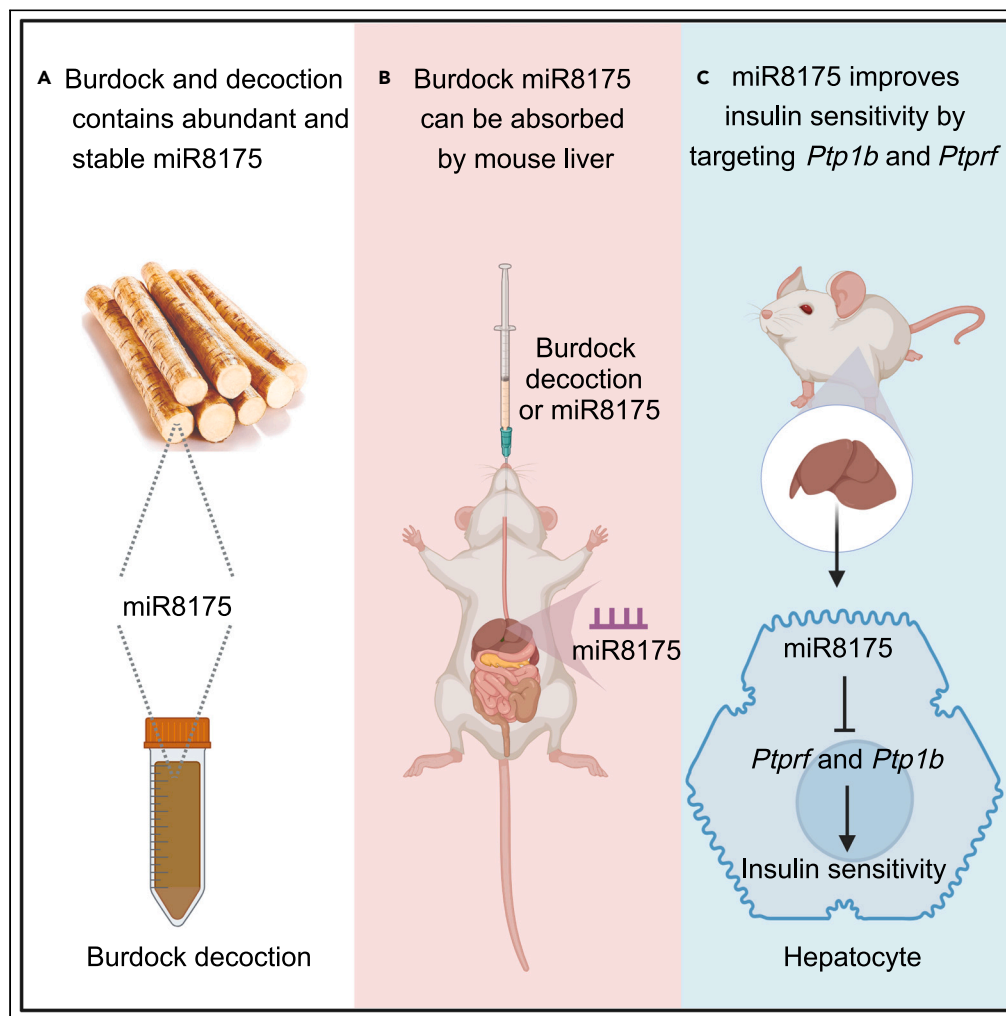


Article

Burdock miR8175 in diet improves insulin resistance induced by obesity in mice through food absorption



Huichen Song, Huanhuan Shi, Mengru Ji, ..., Wen Zhang, Jing Li, Yujing Zhang

111984066@imu.edu.cn (W.Z.)
jingli220@nju.edu.cn (J.L.)
yjjzhang@nju.edu.cn (Y.Z.)

Highlights

Burdock decoction improves insulin sensitivity in diet-induced obese mice

Burdock root contains abundant and stable miR8175

miR8175 can indeed improve insulin sensitivity in diet-induced obese mice

miR8175 improves insulin sensitivity by targeting *Ptp1b* and *Ptp1b*



Article

Burdock miR8175 in diet improves insulin resistance induced by obesity in mice through food absorption

Huichen Song,^{1,2,3,5} Huanhuan Shi,^{1,2,5} Mengru Ji,^{1,2,5} Jiaqi Ding,^{1,2} Lin Cong,^{1,2} Silin Chen,^{1,2} Jiahui Zhou,^{1,2} Xinyan Zha,^{1,2} Jinyang Ye,¹ Runcheng Li,¹ Xiaoyu Hou,¹ Siyu Mao,¹ Xiaohong Jiang,^{1,2} Wen Zhang,^{4,*} Jing Li,^{1,2,*} and Yujing Zhang^{1,2,6,*}

SUMMARY

The incidence of type 2 diabetes mellitus (T2DM) induced by obesity is rapidly increasing. Although there are many synthetic drugs for treating T2DM, they have various side effects. Here, we report that miR8175, a plant miRNA from burdock root, has effective antidiabetic activity. After administration of burdock decoction or synthetic miR8175 by gavage, both burdock decoction and miR8175 can significantly improve the impaired glucose metabolism of diabetic mice induced by a high-fat diet (HFD). Our results demonstrate that burdock decoction and miR8175 enhance the insulin sensitivity of the hepatic insulin signaling pathway by targeting *Ptprf* and *Ptp1b*, which may be the reason for the improvement in metabolism. This study provides a theoretical basis for the main active component and molecular mechanism of burdock to improve insulin resistance. And the study also suggests that plant miRNA may be an indispensable nutrient for maintaining human health.

INTRODUCTION

Type 2 diabetes (T2DM) is a complex chronic disease that is characterized by increased hyperglycemia caused by insulin resistance. More than 400 million people worldwide suffer from T2DM.^{1–3} Currently, many synthetic drugs are used for the therapy of T2DM,^{4–6} and the side effects are not negligible, such as sulfonylureas. Sulfonylurea drugs carry the risk of weight gain and hypoglycemic episodes.⁷ At present, metformin is widely used in the treatment of type 2 diabetes. However, about 30% of people are intolerant to metformin, and over 20% of patients experience side effects, including gastrointestinal side effects.^{8–10} In contrast, traditional Chinese medicine with good efficacy and low toxicity has shown its superiority in the treatment of chronic diseases.^{11–13} Among them, burdock exhibits effective antidiabetic activity.

Burdock (*Arctium lappa*) is a traditional Chinese herbal medicine. It is non-toxic and nutritious and can be used as a daily diet in Asian countries, such as China, Korea, and Japan. Burdock has a variety of pharmacological effects, such as anti-inflammatory, anti-viral, anti-cancer, anti-diabetes and so on, known as the eastern ginseng.^{14–20} There is a long history of using burdock to treat diabetes in China.²¹ Many studies have demonstrated that the burdock root is possibly responsible for the hypoglycemic effect, which was confirmed by the anti-diabetic activity of burdock root found in several subsequent studies.^{16,22,23} However, the molecular mechanism by which burdock root improves diabetes is not well understood.

Recently, studies have suggested that plant microRNAs can enter into the mammalian circulation and organs to regulate gene expression.^{24,25} MiR168 from rice can enter into mouse liver and suppress the expression of low-density lipoprotein receptor adapter protein 1 (LDLRAP1).²⁶ The miR2911 derived from honeysuckle can be effectively absorbed by mice and significantly accumulated in the lung tissue, in which miR2911 directly targets various influenza A subtypes and SARS-CoV-2.^{27,28} The Honeysuckle-derived miR2911 exhibited an anti-tumor effect in colon cancer by specifically targeting the TGF- β 1 mRNA.²⁹ Additionally, Chin et al. found plant miR-159 in human serum, and its abundance was negatively related to the incidence and progression of breast cancer.³⁰ Given these findings, we hypothesize that the plant miRNAs from burdock may be effective components exerting antidiabetic activity.

In this study, we intend to explore the effective components in burdock miRNA that can improve insulin sensitivity. We will use Solexa sequencing to screen for miRNAs that are rich and stably present in Burdock root. Then, we will feed the mice with burdock decoction

¹Nanjing Drum Tower Hospital Center of Molecular Diagnostic and Therapy, State Key Laboratory of Pharmaceutical Biotechnology, Jiangsu Engineering Research Center for MicroRNA Biology and Biotechnology, School of Life Sciences, NJU Advanced Institute of Life Sciences (NAILS), Institute of Artificial Intelligence Biomedicine, Nanjing University, Nanjing 210023, China

²Chinese Academy of Medical Sciences, Research Unit of Extracellular RNA, Nanjing 210023, China

³Department of Urology, Drum Tower Hospital, Medical School of Nanjing University; Institute of Urology, Nanjing University, Nanjing, Jiangsu 210008, P.R. China

⁴Institutes of Biomedical Sciences of Inner Mongolia University, Inner Mongolia 010020, China

⁵These authors contributed equally

⁶Lead contact

*Correspondence: 111984066@imu.edu.cn (W.Z.), jingli220@nju.edu.cn (J.L.), yjzhang@nju.edu.cn (Y.Z.)
<https://doi.org/10.1016/j.isci.2024.109705>



and chemically synthesized miRNA to demonstrate whether the screened burdock miRNA can be absorbed by mice and delivered to target tissues. Furthermore, by only feeding the selected miRNA, we will investigate whether it has an independent effect on improving insulin sensitivity. After predicting the target genes of this miRNA, we will further verify its direct regulatory effect on the target genes, thereby elucidating the molecular mechanism by which this miRNA in burdock improves insulin sensitivity.

RESULTS

Burdock decoction can improve insulin resistance in diet-induced obese mice

To verify whether burdock root decoction improves insulin resistance in obese mice, we induced a DIO mouse model by continuously feeding 4-week-old C57BL/6j mice with a high-fat diet for 8 weeks (Figures S1A–S1C). Then, the DIO mice were each orally administered with burdock root decoction or sterile water for six consecutive weeks (500 μ L/day, $n = 8$ in each group) (Figure 1A). We observed that the mice who received the burdock decoction ($n = 8$) did not show a significant decrease in weight compared with sterile water group ($n = 8$) (Figure 1B). However, their fasting blood glucose showed decrease from the fourth week, reaching a significant difference after six weeks' administration (Figure 1C). We further assessed the metabolic profile with fasting blood lipids and insulin levels in burdock decoction treated mice. The results showed that TG and insulin levels significantly decreased (Figures 1D and 1H), while T-CHO (Figure 1E), HDL (Figure 1F), and LDL (Figure 1G) levels all remained unchanged. Besides, glucose tolerance test (GTT) and insulin tolerance test (ITT) results demonstrated that the insulin sensitivity of DIO mice administered with burdock decoction was significantly improved (Figures 1I and 1J). These results indicate that burdock root decoction can indeed restore insulin sensitivity in DIO mice.

Screening of active miRNAs via high-throughput sequencing

Because plant miRNA may be one of the active components of traditional Chinese medicine, we extracted total small RNA from burdock roots to explore whether miRNAs in burdock decoction participate in promoting insulin sensitivity in DIO mice. We then used Illumina deep-sequencing technology to search for the most abundant miRNAs in burdock roots. According to the sequencing data, we found that ath-miR8175 and gma-miR6300 were particularly abundant in burdock roots (Figure 2A). Q-PCR was used to validate these results (Figure 2B). Interestingly, we found that miR8175 displayed particularly stable characteristics during the process of obtaining burdock decoction via high-temperature steaming. Its level was 100 times higher than that of miR6300 (Figure 2C). At the same time, we found that the sequence of miR8175 has high GC content (about 75%), which is similar to the GC content of miR2911, the active ingredient of honeysuckle²⁷ (Figure 2D). Therefore, we selected the most abundant and stable miR8175 as the main research target.

MiR8175 can be absorbed by gavage feeding

Can miR8175 in burdock decoction be absorbed through the gavage feeding and reach the body to work? In order to solve this problem, the normal C57 mice were given 500 μ L burdock decoction by gavage ($n = 5$), and detected the level of miR8175 in serum and insulin-sensitive tissues such as liver, skeletal muscle, and adipose tissue after 0, 3, 6, 9, and 12 h to determine whether miR8175 could be absorbed into the blood via diet and reach these tissues (Figure 3A). According to the results, we found that after gavage with burdock decoction, the level of miR8175 indeed increased in serum, reaching its peak at 6 h and still exhibiting significant differences at 12 h, indicating that miR8175 could be absorbed into the blood via diet (Figure 3B). In addition, miR8175 showed a significant increase in liver from 3h, and this increase could even last until 12h, while the increase in muscle or adipose tissue was not significant (Figures 3C–3E). At the same time, mice were given 1nmol synthetic miR8175 in the same way (Figure 3F). The trend of miR8175's increase in tissues in mice gavaged with synthesized miR8175 was similar to that of burdock decoction group, except that the peak in serum appeared at 3 h (Figures 3G–3J). These results indicate that miR8175 absorbed via gavage maybe more easily enriched in the liver and which was further confirmed by gavage feeding of Cy3-labeled miR8175 (Figure 3K). We tracked the tissue distribution of miR8175 after gavage Cy3-miR8175 and found that the liver was still the main site of miR8175 enrichment (Figure 3L). Furthermore, we detected the distribution of miR8175 in serum and found that miR8175 mainly exists in extracellular vesicles, suggesting that it may be delivered to the liver via extracellular vesicles after gavage (Figures 3M and 3N).

Gavage with miR8175 can improve insulin sensitivity in DIO mice

To further investigate whether the most abundant miR8175 in burdock decoction can improve insulin sensitivity in DIO mice, we gavaged DIO mice with 1 nmol miR8175 or negative control RNA (NC group, $n = 8$) for 6 weeks and detected their body weight and fasting glucose every week (Figure 4A). We found that their body weight decreased slightly during the gavage process (Figure 4B), and fasting glucose began to decrease significantly from 3 weeks and had a more significant effect by 6w (Figure 4C). However, the blood lipid level at 6w did not change significantly (Figures S2A–S2D). The insulin level decreased significantly after gavage for 6w (Figure 4D), and the results of GTT and ITT experiments suggested a significant improvement in insulin sensitivity (Figures 4E and 4F). In obese mice, islets produce compensatory hyperplasia to increase insulin production and maintain blood sugar balance. As the islet β cells are unable to maintain the glucose metabolic load, the islets become hypertrophic, malformed, and even disintegrated.³¹ With the use of gadofullerene nanoparticles to reverse islet dysfunction, Li et al. found that GFNPs can effectively alleviate islet damage, reduce compensatory hyperplasia of islets, and maintain the function of islet beta cells during the treatment of hepatic insulin resistance.³² Therefore, in order to further clarify whether miR8175 also reduces the damage to islets and alleviates the compensatory increase of islets in the process of improving insulin resistance, we tested the size and

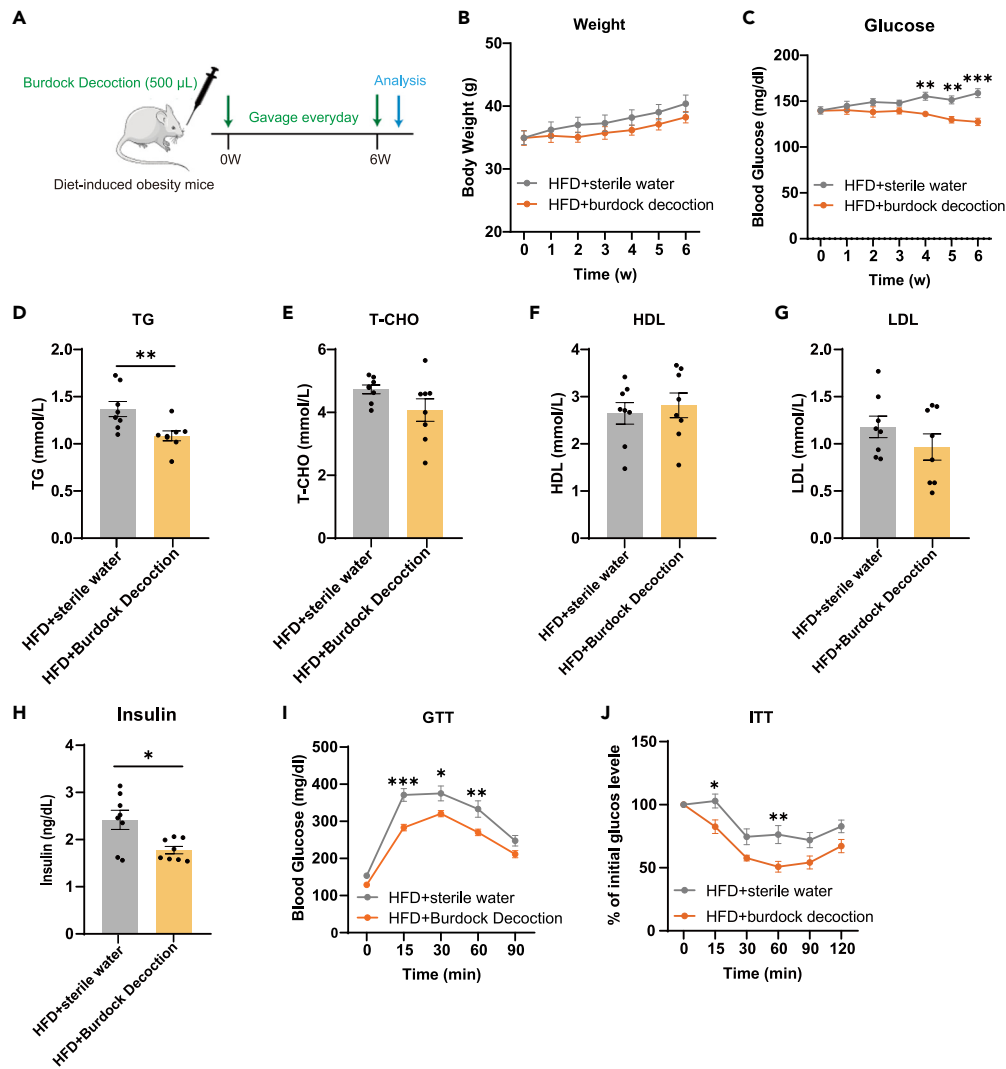


Figure 1. Burdock decoction improves insulin sensitivity in diet-induced obese mice

(A) Experimental scheme.

(B) Body weight and (C) fasting blood glucose were measured weekly.

(D–G) The levels of TG (D), TC (E), HDL (F), and LDL (G) in serum were measured.

(H) The levels of insulin in serum were measured.

(I, J) Glucose tolerance (I) and insulin tolerance (J) were tested. Data are presented as mean \pm SEM. * $p < 0.05$, ** $p < 0.01$, and *** $p < 0.001$; two-way ANOVA (B–C, I–J) or Student's *t* test (D–H).

number of islets after treatment with miR8175. Our results showed that without changing the number of islets, the treatment of miR8175 effectively alleviates the compensatory hyperplasia of islets, suggesting that the treatment of miR8175 can reduce the functional damage of islets. (Figures 4G–4I).

To further investigate how miR8175 improves insulin sensitivity in tissues, we first examined which tissues miR8175 is enriched in. The results showed that the miR8175 was enriched in liver of miR8175 treated DIO mice (Figure 5A), while in muscle and adipose tissue were still not significant (Figures 5B and 5C). Then we performed transcriptome sequencing on the livers of both groups of mice, and the sequencing results were uploaded to GEO database (GEO: GSE248220). Through data analysis, gavage of miR8175 changed the expression of many genes (Figure 5D). GSEA analysis showed that the up-regulated genes were mainly concentrated in regulation of glucose metabolic process (Figure 5E). In the insulin signaling pathway in the liver, insulin binds to the insulin receptor, activating downstream pathways through PI3K-mediated phosphorylation of AKT.³³ The level of phosphorylated AKT under insulin stimulation reflects the activation of the insulin signaling pathway. We further investigated insulin sensitivity in liver caused by miR8175 treatment. The results showed that the AKT phosphorylation level after insulin stimulation was significantly increased in the miR8175 treated group, indicating that miR8175 had indeed improved the insulin sensitivity of liver tissue (Figure 5F).

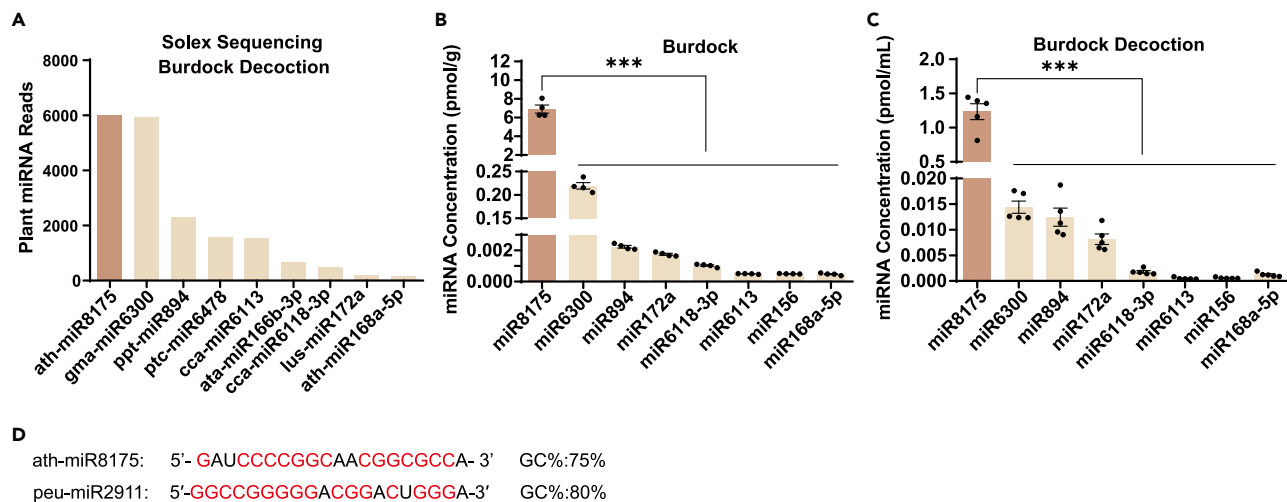


Figure 2. miR8175 is highly enriched in burdock decoction

(A) The sequencing reads of plant miRNAs in burdock decoction.

(B and C) The concentrations of plant miRNAs were detected by qRT-PCR: (B) burdock (n = 4); (C) burdock decoction (n = 5); (D) The sequence and GC content of miR8175 and miR2911. Data are presented as mean \pm SEM. *p < 0.05, **p < 0.01, and ***p < 0.001; one-way ANOVA (B-C).

MiR8175 improves insulin sensitivity by targeting *Ptprf* and *Ptp1b*

To further explore how miR8175 improved the insulin sensitivity of liver tissue, we performed miRNA pull-down assay to analyze mRNAs bound to miR8175. Biotin-labeled miR8175 was transfected into Hepa1-6 cells, and then miR8175 was pull-down by magnetic bead method, the bound mRNAs were eluted to RNA sequencing. The specific process can be seen in Figure 6A. We identified 3769 genes that bind to miR8175. Subsequently, in order to further screen which of these genes are the target genes directly affected by miR8175, we predicted the target genes of miR8175 in mice through RNAhybrid, and then interacted with the pull-downed mRNA to obtain a total of 1990 possible target gene sets (Figure 6B). Subsequent KEGG pathway analysis of these genes found that the target genes were mainly concentrated in some anti-tumor (green labeled pathway) and anti-viral (blue labeled pathway), which was consistent with the reported anti-tumor and anti-viral efficacy of Burdock (Figure 6C). The pathway related to the regulation of glucose metabolism is the insulin signaling pathway (Figure 6C). In the target genes of this pathway, we found three target genes, *Ptprf*,³⁴ *Ptpn1*,^{35,36} and *Socs3*,^{37,38} which have been reported to be negatively correlated with insulin sensitivity (Figures 6C and 6D). To verify the accuracy of the predicted target proteins, we checked the expression levels of these proteins in liver tissue after long-term intragastric miR8175 feeding and found that PTPRF, PTP1B and SOCS3 were significantly down-regulated (Figure 6E). Furthermore, we verified the changes in PTPRF and PTP1B by transfecting liver cells with miR8175, indicating that the reduced expression levels of SOCS3 in mouse liver may be caused by other factors in the body (Figure 6F). To further verify whether these target genes were directly regulated by miR8175, we constructed luciferase vectors with predicted binding sites or mutated binding sites of these target genes, and detected the effect of miR8175 on luciferase activity. The results showed that miR8175 significantly reduced the expression of luciferase containing the target gene binding site of both *Ptprf* and *Ptp1b*, but had no effect on luciferase activity after the seed sequence binding site was mutated (Figures 6G and 6H). These results further indicated that *Ptprf* and *Ptp1b* are direct targets of miR8175. Since the increase of PTP1B and PTPRF under obese conditions can inhibit tissue insulin sensitivity by dephosphorylating IR and IRS,^{6,34,39} we further verified the phosphorylation levels of IR and IRS in liver tissue after insulin stimulation of miR8175 treated groups. The results showed that the insulin-stimulated phosphorylation levels of IR and IRS in DIO mice fed with miR8175 were significantly increased (Figure 6I), indicating that long-term intragastric miR8175 may directly inhibit the increase of PTP1B and PTPRF, reduced dephosphorylation levels of p-IR and p-IRS, and improve insulin sensitivity in mice.

DISCUSSION

Traditional Chinese medicine has been favored due to its good therapeutic effects and small side effects, especially many medicinal foods and herbs that can be used as daily food, such as burdock, which is one of the popular foods in Central Asia. Research has shown that burdock has anti-inflammatory, anti-tumor, anti-virus, blood glucose-lowering, and lipid-lowering effects. However, due to its unclear medicinal mechanism, its widespread promotion as a medicinal herb is limited, and it can only be promoted as a health food. In this study, we have also confirmed that burdock decoction can effectively improve insulin resistance in DIO mice (Figure 1). To explore its mechanism of action, this article mainly investigates the molecular mechanism of burdock decoction in improving obesity-induced insulin resistance from the perspective of plant miRNA. This study provides a reference for the mechanism of traditional Chinese medicine in treating diabetes, offering a basis for clinical application and providing more possibilities for the treatment of diabetes.

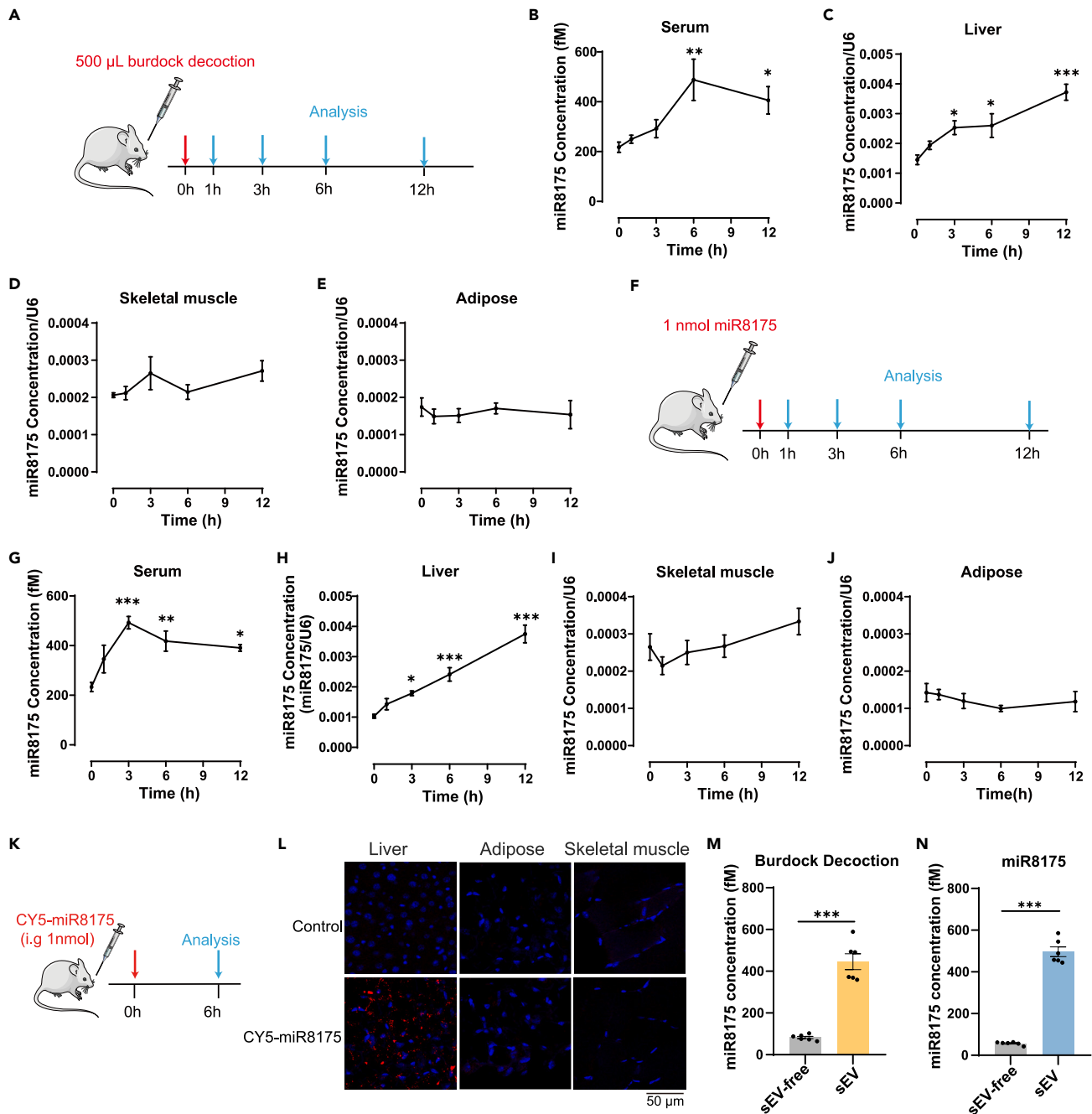


Figure 3. miR8175 is delivered into mouse liver following burdock decoction or miR8175 gavage administration

(A) Experimental scheme. (B–E) After gavage-feeding burdock decoction, the kinetics of miR8175 were detected by qRT-PCR: (B) serum ($n = 5$); (C) liver ($n = 5$); (D) skeletal muscle ($n = 5$); (E) adipose ($n = 5$). (F) Experimental scheme. (G–J) After gavage-feeding 500 pmol synthetic miR8175 in 500 μ L of RNase-free water, the miR8175 kinetics were detected by qRT-PCR: (G) serum ($n = 5$); (H) liver ($n = 5$); (I) skeletal muscle ($n = 5$); (J) adipose ($n = 5$).

(K) Experimental scheme.

(L) Confocal microscopy photos of mouse liver 3 h after administration of 1 nmol synthetic, fluorescently labeled miR8175 by gavage, scale bar: 50 μ m.

(M and N) qPCR analysis of the miR8175 concentration in the exosome-free plasma fraction or exosomal fraction isolated from the plasma gavage fed with (M) burdock decoction or (N) synthetic miR8175 ($n = 6$). Data are presented as mean \pm SEM. * $p < 0.05$, ** $p < 0.01$, and *** $p < 0.001$; Student's t test (M–N) or one-way ANOVA (B–E, G–J).

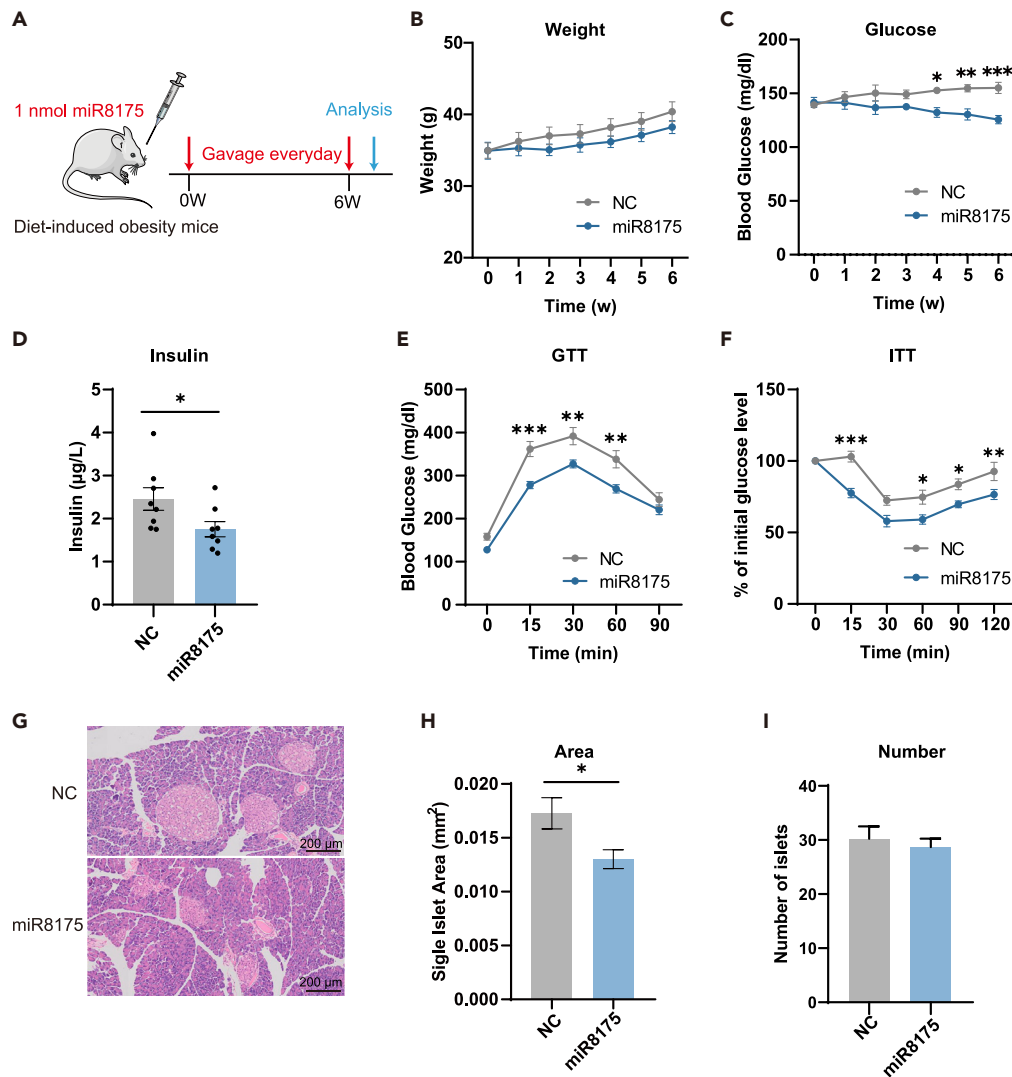


Figure 4. miR8175 improves insulin sensitivity in diet-induced obese mice

(A) Experimental scheme.

(B) Body weight and (C) fasting blood glucose were measured weekly.

(D) The levels of insulin in serum were measured.

(E and F) Glucose tolerance (E) and insulin tolerance (F) were tested; (G) Representative images of H&E staining of pancreas, scale bar: 200 µm.

(H) The average single islet area and (I) the number of single islets in the pancreas. $n = 8$. Data are presented as mean \pm SEM. * $p < 0.05$, ** $p < 0.01$, and *** $p < 0.001$; two-way ANOVA (B–C, E–F) or Student's t test (D, H–I).

We found that miR8175, which is very rich in expression in burdock root as revealed by Solexa sequencing, and very high GC content which attracted our attention. Like miR2911 of honeysuckle, which we previously found capable of targeting influenza virus in our preliminary study,²⁷ it also has particularly high GC content and exhibits strong stability such as resistance to high temperature, acid and alkali. MiR8175 also exhibits the same stability. We found that in burdock decoction made by high-temperature cooking of burdock roots, miR8175 displayed characteristics of high abundance and high stability compared to other miRNAs (Figures 2A–2C). This stability means that miR8175 can be an appropriate drug-effective ingredient. After gavage administration, we observed that the level of miR8175 in liver cells reached 300 copies/cell, which also indicated that miR8175 had reached the level to play a physiological function. The fact that the levels of the target genes *Ptprf* and *Ptp1b* in liver tissue decreased by 2-fold and 3-fold, respectively, after long-term treatment with miR8175, further confirmed this point.

In the predicted target genes of miR8175, we found many PTP family proteins, such as PTP1B, PTPN11, PTPRF, and PTPA. These PTP family proteins play an important role in the dephosphorylation of proteins.⁴⁰ PTP1B, PTPRF, SHP1 and SHP2 have been reported to increase insulin resistance by dephosphorylating the phosphorylation level of p-IR and p-IRS.⁴¹ Moreover, many studies have developed drugs that promote insulin signaling pathways sensitivity targeting PTP family proteins.^{42–45} In this study, we have confirmed that miR8175 plays a role in

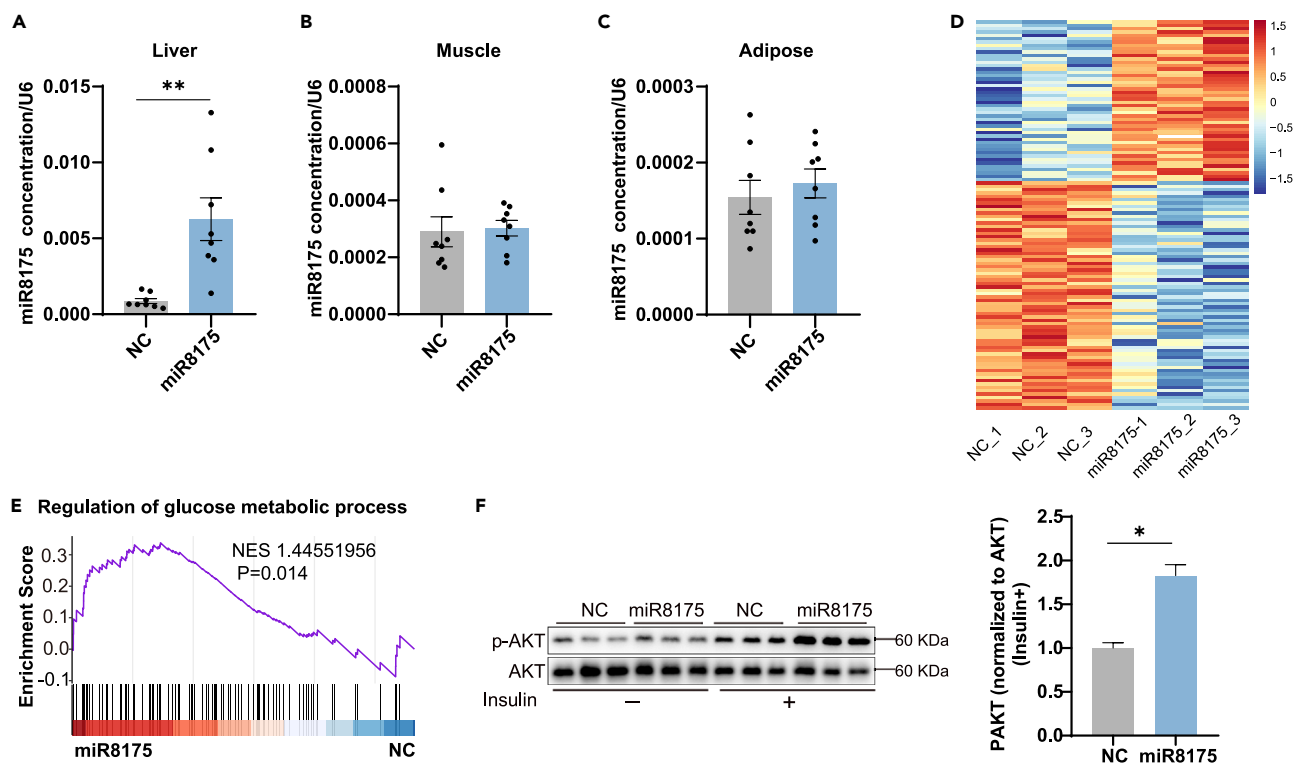


Figure 5. miR8175 regulates glucose metabolism in the liver

(A–C) qPCR analysis of the miR8175 concentration in the (A) liver, (B) skeletal muscle and (C) adipose of mice gavage fed with synthetic miR8175 ($n = 8$).

(D) Heatmap analysis of differential mRNA expression in mouse liver following NC and miR8175 gavage administration.

(E) Gene Set Enrichment Analysis (GSEA) of regulation of glucose metabolism process in mouse liver following NC and miR8175 gavage administration; (F) Western blotting and densitometry analysis of insulin-stimulated phosphorylated AKT and total AKT in mouse liver following NC and miR8175 gavage administration. Data are presented as mean \pm SEM. * $p < 0.05$, ** $p < 0.01$, and *** $p < 0.001$; or Student's t test (A–C, F).

promoting insulin signaling pathway sensitivity by directly inhibiting PTP1B and PTPRF levels, making it a very promising drug molecule to improve insulin signaling pathway sensitivity (Figure 7).

In addition, when predicting the target genes of miR8175, we found by KEGG pathway analysis that many target genes of miR8175 were enriched in cancer-related signaling pathways, such as the estrogen signaling pathway, which is one of the main factors leading to breast cancer. Important target genes such as ESR1, ESRRA, ESRRB, and ESRRG, which are estrogen receptor-related proteins, and CDK4 and CDK6, which are cell cycle-related proteins, were downregulated, which may become a potential therapeutic method for breast cancer. The presence of some target genes related to tumors, such as BRAF, also suggests that miR8175 may have the potential to be an effective functional molecule in burdock for treating tumors, although this still needs further experimental verification.

Overall, we once again confirmed that burdock root decoction can effectively improve high-fat diet-induced insulin resistance, and identified miR8175 as a key miRNA molecule that can play a critical role. By investigating the direct regulatory role of miR8175 on the target genes *Ptprf* and *Ptp1b*, we revealed that miR8175 can enhance the sensitivity of insulin signaling pathways by targeting of *Ptprf* and *Ptp1b*, which dephosphorylate p-IR and p-IRS, respectively.

In this study, we found miR8175 is the functional miRNA in burdock, which can be absorbed by mice and can improve glucose metabolism. In this study, miR8175, a plant microRNA from burdock decoction that plays a role in anti-diabetic, was screened. Further studies have shown that miR8175 can inhibit the dephosphorylation levels of p-IR and p-IRS by targeting PTP1B and PTPRF, increase the sensitivity of insulin signaling pathway. This will help in designing safer and more effective herbal medicines, conducting and promoting clinical trials of traditional Chinese medicine, providing scientific basis for the development and utilization of traditional Chinese medicine, and facilitating the integration of traditional Chinese medicine with modern medicine. In addition, this study also provides a theoretical basis for the cross-kingdom regulation of plant miRNA.

Our research results have two implications in clinical applications.

- (1) Using miR8175 to improve obesity-related insulin sensitivity;
- (2) Promoting the exploration of effective miRNAs in traditional Chinese medicine to facilitate the development of traditional Chinese medicine.

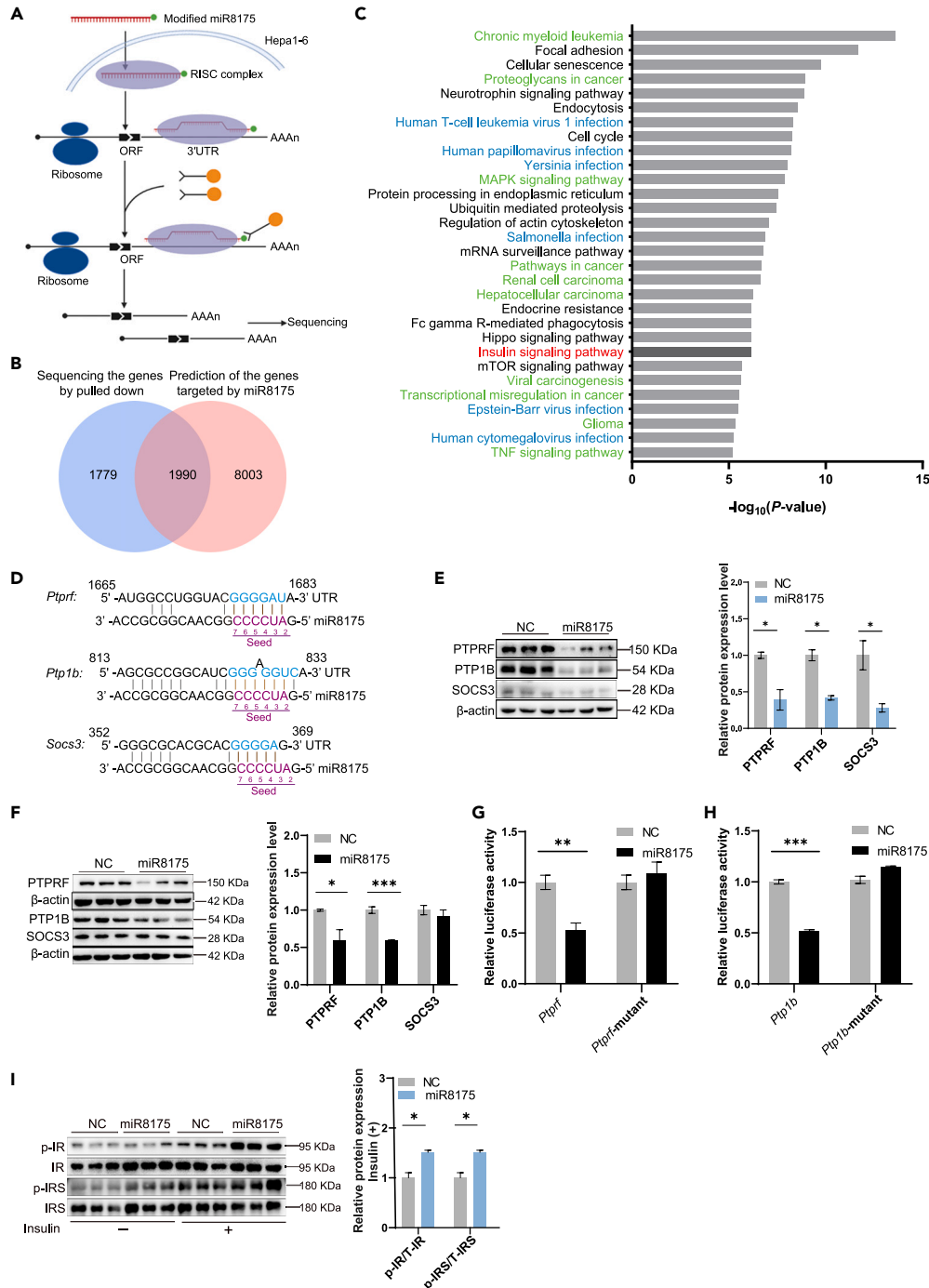


Figure 6. miR8175 improves insulin sensitivity by targeting *Ptp1b* and *Ptp1b*

(A) Experimental scheme.

(B) Overlapping target genes between IP-sequenced genes and software-predicted targets.

(C) KEGG analysis of the 1990 DEGs in these datasets. The top 30 pathways shown based on the pvalue; (D) Prediction of the genome sequence targeted by miR8175.

(E) Western blotting and densitometry analysis of PTPRF, PTP1B, SOCS3 protein levels in mouse liver following NC and miR8175 gavage administration.

(F) Western blotting and densitometry analysis of the PTPRF, PTP1B, SOCS3, protein levels in Hepa1-6 cell after transfecting miR8175 or ncRNA (G, H). Dual luciferase reporter activities after transfecting 239T cells with miR8175 and reporter carrying 3' UTR in the long form of (G) *Ptp1b* and (H) *Ptp1b*.

(I) Western blotting and densitometry analysis of insulin-stimulated phosphorylated IR, total IR, phosphorylated IRS, total IRS in mouse liver following NC and miR8175 gavage administration. Data are presented as mean \pm SEM. * $p < 0.05$, ** $p < 0.01$, and *** $p < 0.001$; Student's t test (E–I).

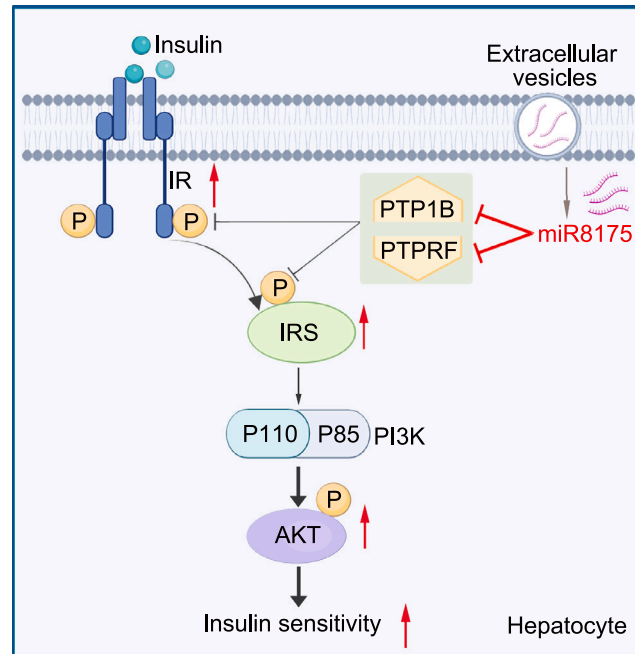


Figure 7. Graphic illustration of the miR8175 targeting pathway in hepatocytes

MiR8175 promotes insulin sensitivity by targeting *Ptprf* and *Ptp1b* to promote IR and IRS phosphorylation. Figure created using BioRender.

Limitations of the study

The mechanism by which miR8175 is absorbed by mice and how it is delivered to target tissues was not directly demonstrated in this study. Based on preliminary research in the laboratory (Chen et al., 2021), it is suggested that miR8175 might be internalized by SIDT1 protein on the gastric pit cells after entering the stomach, and then encapsulated into vesicles and secreted to other tissues or organs in the form of exosomes. However, in this study, we did not provide experimental evidence to further confirm this.

STAR★METHODS

Detailed methods are provided in the online version of this paper and include the following:

- [KEY RESOURCES TABLE](#)
- [RESOURCE AVAILABILITY](#)
 - Lead contact
 - Materials availability
 - Data and code availability
- [EXPERIMENTAL MODEL AND STUDY PARTICIPANT DETAILS](#)
 - Animal
 - Cell
- [METHOD DETAILS](#)
 - Burdock decoction
 - RNA extraction
 - RNA extraction from serum and tissues
 - qRT-PCR of plant microRNA
 - Illumina deep sequencing
 - Pull-down experiment
 - RNA-seq library preparation and sequencing
 - Western blot
 - Glucose tolerance test and insulin tolerance test
 - Evaluate insulin sensitivity in mouse liver
 - Histopathological examination of pancreatic tissue
 - sEV isolation

- Plasmid conduction and luciferase assay
- **QUANTIFICATION AND STATISTICAL ANALYSIS**

SUPPLEMENTAL INFORMATION

Supplemental information can be found online at <https://doi.org/10.1016/j.isci.2024.109705>.

ACKNOWLEDGMENTS

This work was supported by the CAMS Innovation Fund for Medical Sciences (No. CIFMS-2021-I2M-5-015), National Natural Science Foundation of China (No. 31771666 and 31972912), Natural Science Foundation of Inner Mongolia Autonomous Region (2023QN03012), the Fundamental Research Funds for the Central Universities (No. 020814380173), the Jiangsu Science and Technology Department (No. BK20211153).

AUTHOR CONTRIBUTIONS

Z.Y.J. and L.J., conceived and designed the work. S.H.C. and S.H.H. performed the animal experiments and molecular biology experiments. and J.M.R. and Z.W. analyzed conducted bioinformatics analysis of RNA-seq data. Z.Y.J. and S.H.C. wrote the manuscript. Z.J.H., Z.X.Y., L.R.C., H.X.Y., M.S.Y., and J.X.H. revised the manuscript. All authors have read and approved the final manuscript.

DECLARATION OF INTERESTS

The authors declare no competing interests.

Received: December 18, 2023

Revised: January 23, 2024

Accepted: April 6, 2024

Published: April 9, 2024

REFERENCES

1. Demir, S., Nawroth, P.P., Herzog, S., and Ekim Üstünel, B. (2021). Emerging Targets in Type 2 Diabetes and Diabetic Complications. *Adv. Sci.* 8, e2100275. <https://doi.org/10.1002/adv.202100275>.
2. NCD-, N.R.F.C. (2017). NCD Risk Factor Collaboration (NCD-RisC). Worldwide trends in diabetes since 1980: a pooled analysis of 751 population-based studies with 4.4 million participants (vol 387, pg 1513, 2016). *Lancet* 389, E2. [https://doi.org/10.1016/S0140-6736\(16\)32060-8](https://doi.org/10.1016/S0140-6736(16)32060-8).
3. Sun, H., Saeedi, P., Karuranga, S., Pinkepank, M., Ogurtsova, K., Duncan, B.B., Stein, C., Basit, A., Chan, J.C.N., Mbanya, J.C., et al. (2022). IDF Diabetes Atlas: Global, regional and country-level diabetes prevalence estimates for 2021 and projections for 2045. *Diabetes Res. Clin. Pract.* 183, 109119. <https://doi.org/10.1016/j.diabres.2021.109119>.
4. Phung, O.J., Scholle, J.M., Talwar, M., and Coleman, C.I. (2010). Effect of noninsulin antidiabetic drugs added to metformin therapy on glycemic control, weight gain, and hypoglycemia in type 2 diabetes. *JAMA* 303, 1410–1418. <https://doi.org/10.1001/jama.2010.405>.
5. van Staa, T., Abenham, L., and Monette, J. (1997). Rates of hypoglycemia in users of sulfonylureas. *J. Clin. Epidemiol.* 50, 735–741. [https://doi.org/10.1016/s0895-4356\(97\)00024-3](https://doi.org/10.1016/s0895-4356(97)00024-3).
6. Ahmad, F., Considine, R.V., and Goldstein, B.J. (1995). Increased abundance of the receptor-type protein-tyrosine phosphatase LAR accounts for the elevated insulin receptor dephosphorylating activity in adipose tissue of obese human subjects. *J. Clin. Invest.* 95, 2806–2812. <https://doi.org/10.1172/JCI117985>.
7. Khunti, K., Chatterjee, S., Gerstein, H.C., Zoungas, S., and Davies, M.J. (2018). Do sulphonylureas still have a place in clinical practice? *Lancet Diabetes Endocrinol.* 6, 821–832. [https://doi.org/10.1016/S2213-8587\(18\)30025-1](https://doi.org/10.1016/S2213-8587(18)30025-1).
8. Bonnet, F., and Scheen, A. (2017). Understanding and overcoming metformin gastrointestinal intolerance. *Diabetes Obes. Metabol.* 19, 473–481. <https://doi.org/10.1111/dom.12854>.
9. García-Calzón, S., Perilyev, A., Martinell, M., Ustinova, M., Kalamajski, S., Franks, P.W., Bacos, K., Elbere, I., Pihlajamäki, J., Volkov, P., et al. (2020). Epigenetic markers associated with metformin response and intolerance in drug-naïve patients with type 2 diabetes. *Sci. Transl. Med.* 12, eaaz1803. <https://doi.org/10.1126/scitranslmed.aaz1803>.
10. Cook, M.N., Girman, C.J., Stein, P.P., and Alexander, C.M. (2007). Initial monotherapy with either metformin or sulphonylureas often fails to achieve or maintain current glycaemic goals in patients with Type 2 diabetes in UK primary care. *Diabet. Med.* 24, 350–358. <https://doi.org/10.1111/j.1464-5491.2007.02078.x>.
11. Liu, X.J., Hu, X.K., Yang, H., Gui, L.M., Cai, Z.X., Qi, M.S., and Dai, C.M. (2022). A Review of Traditional Chinese Medicine on Treatment of Diabetic Nephropathy and the Involved Mechanisms. *Am. J. Chin. Med.* 50, 1739–1779. <https://doi.org/10.1142/S0192415X22500744>.
12. Wang, X., Zhang, J., He, S., Gao, Y., Ma, X., Gao, Y., Zhang, G., Kui, L., Wang, W., Wang, Y., et al. (2018). HMOD: An Omics Database for Herbal Medicine Plants. *Mol. Plant* 11, 757–759. <https://doi.org/10.1016/j.molp.2018.03.002>.
13. Chi, J., Sun, L., Cai, L., Fan, L., Shao, C., Shang, L., and Zhao, Y. (2021). Chinese herb microneedle patch for wound healing. *Bioact. Mater.* 6, 3507–3514. <https://doi.org/10.1016/j.bioactmat.2021.03.023>.
14. Yosri, N., Alsharif, S.M., Xiao, J., Musharraf, S.G., Zhao, C., Saeed, A., Gao, R., Said, N.S., Di Minno, A., Daglia, M., et al. (2023). Arctium lappa (Burdock): Insights from ethnopharmacology potential, chemical constituents, clinical studies, pharmacological utility and nanomedicine. *Biomed. Pharmacother.* 158, 114104. <https://doi.org/10.1016/j.biopha.2022.114104>.
15. Gao, Y., Gu, C., Wang, K., Wang, H., Ruan, K., Xu, Z., and Feng, Y. (2018). The effects of hypoglycemia and weight loss of total lignans from Fructus Arctii in KKAY mice and its mechanisms of the activity. *Phytother. Res.* 32, 631–642. <https://doi.org/10.1002/ptr.6003>.
16. Tusch, D., Bidet, L.P.R., Cazals, G., Ferrare, K., Leroy, J., Faucanié, M., Chevassus, H., Tournier, M., Lajoix, A.D., and Azay-Milhau, J. (2014). Chemical analysis and antihyperglycemic activity of an original extract from burdock root (Arctium lappa). *J. Agric. Food Chem.* 62, 7738–7745. <https://doi.org/10.1021/jf500926v>.
17. Awale, S., Lu, J., Kalauni, S.K., Kurashima, Y., Tezuka, Y., Kadota, S., and Esumi, H. (2006). Identification of arctigenin as an antitumor agent having the ability to eliminate the tolerance of cancer cells to nutrient starvation. *Cancer Res.* 66, 1751–1757. <https://doi.org/10.1158/0008-5472.CAN-05-3143>.

18. Chen, J., Li, W., Jin, E., He, Q., Yan, W., Yang, H., Gong, S., Guo, Y., Fu, S., Chen, X., et al. (2016). The antiviral activity of arctigenin in traditional Chinese medicine on porcine circovirus type 2. *Res. Vet. Sci.* 106, 159–164. <https://doi.org/10.1016/j.rvsc.2015.10.012>.
19. Li, H., Zhang, X., Xiang, C., Feng, C., Fan, C., Liu, M., Lu, H., Su, H., Zhou, Y., Qi, Q., et al. (2021). Identification of phosphodiesterase-4 as the therapeutic target of arctigenin in alleviating psoriatic skin inflammation. *J. Adv. Res.* 33, 241–251. <https://doi.org/10.1016/j.jare.2021.02.006>.
20. Tsai, W.J., Chang, C.T., Wang, G.J., Lee, T.H., Chang, S.F., Lu, S.C., and Kuo, Y.C. (2011). Arctigenin from *Arctium lappa* inhibits interleukin-2 and interferon gene expression in primary human T lymphocytes. *Chin. Med.* 6, 12. <https://doi.org/10.1186/1749-8546-6-12>.
21. Chan, Y.S., Cheng, L.N., Wu, J.H., Chan, E., Kwan, Y.W., Lee, S.M.Y., Leung, G.P.H., Yu, P.H.F., and Chan, S.W. (2011). A review of the pharmacological effects of *Arctium lappa* (burdock). *Inflammopharmacology* 19, 245–254. <https://doi.org/10.1007/s10787-010-0062-4>.
22. Annunziata, G., Barrea, L., Ciampaglia, R., Cicala, C., Arnone, A., Savastano, S., Nabavi, S.M., Tenore, G.C., and Novellino, E. (2019). *Arctium lappa* contributes to the management of type 2 diabetes mellitus by regulating glucose homeostasis and improving oxidative stress: A critical review of in vitro and in vivo animal-based studies. *Phytother. Res.* 33, 2213–2220. <https://doi.org/10.1002/ptr.6416>.
23. Ferracane, R., Graziani, G., Gallo, M., Fogliano, V., and Ritieni, A. (2010). Metabolic profile of the bioactive compounds of burdock (*Arctium lappa*) seeds, roots and leaves. *J. Pharm. Biomed. Anal.* 51, 399–404. <https://doi.org/10.1016/j.jpba.2009.03.018>.
24. Zhao, Y., Cong, L., and Lukiw, W.J. (2018). Plant and Animal microRNAs (miRNAs) and Their Potential for Inter-kingdom Communication. *Cell. Mol. Neurobiol.* 38, 133–140. <https://doi.org/10.1007/s10571-017-0547-4>.
25. Chen, Q., Zhang, F., Dong, L., Wu, H., Xu, J., Li, H., Wang, J., Zhou, Z., Liu, C., Wang, Y., et al. (2021). SIDT1-dependent absorption in the stomach mediates host uptake of dietary and orally administered microRNAs. *Cell Res.* 31, 247–258. <https://doi.org/10.1038/s41422-020-0389-3>.
26. Zhang, L., Hou, D., Chen, X., Li, D., Zhu, L., Zhang, Y., Li, J., Bian, Z., Liang, X., Cai, X., et al. (2012). Exogenous plant MIR168a specifically targets mammalian LDLRAP1: evidence of cross-kingdom regulation by microRNA. *Cell Res.* 22, 107–126. <https://doi.org/10.1038/cr.2011.158>.
27. Zhou, Z., Li, X., Liu, J., Dong, L., Chen, Q., Liu, J., Kong, H., Zhang, Q., Qi, X., Hou, D., et al. (2015). Honeysuckle-encoded atypical microRNA2911 directly targets influenza A viruses. *Cell Res.* 25, 39–49. <https://doi.org/10.1038/cr.2014.130>.
28. Zhou, L.K., Zhou, Z., Jiang, X.M., Zheng, Y., Chen, X., Fu, Z., Xiao, G., Zhang, C.Y., Zhang, L.K., and Yi, Y. (2020). Absorbed plant MIR2911 in honeysuckle decoction inhibits SARS-CoV-2 replication and accelerates the negative conversion of infected patients. *Cell Discov.* 6, 54. <https://doi.org/10.1038/s41421-020-00197-3>.
29. Liu, C., Xu, M., Yan, L., Wang, Y., Zhou, Z., Wang, S., Sun, Y., Zhang, J., and Dong, L. (2021). Honeysuckle-derived microRNA2911 inhibits tumor growth by targeting TGF-beta1. *Chin. Med.* 16, 49. <https://doi.org/10.1186/s13020-021-00453-y>.
30. Chin, A.R., Fong, M.Y., Somlo, G., Wu, J., Swiderski, P., Wu, X., and Wang, S.E. (2016). Cross-kingdom inhibition of breast cancer growth by plant miR159. *Cell Res.* 26, 217–228. <https://doi.org/10.1038/cr.2016.13>.
31. Rhodes, C.J. (2005). Type 2 diabetes—a matter of beta-cell life and death? *Science* 307, 380–384. <https://doi.org/10.1126/science.1104345>.
32. Li, X., Zhen, M., Zhou, C., Deng, R., Yu, T., Wu, Y., Shu, C., Wang, C., and Bai, C. (2019). Gadofullerene Nanoparticles Reverse Dysfunctions of Pancreas and Improve Hepatic Insulin Resistance for Type 2 Diabetes Mellitus Treatment. *ACS Nano* 13, 8597–8608. <https://doi.org/10.1021/acsnano.9b02050>.
33. Haeusler, R.A., McGraw, T.E., and Accili, D. (2018). Biochemical and cellular properties of insulin receptor signalling. *Nat. Rev. Mol. Cell Biol.* 19, 31–44. <https://doi.org/10.1038/nrm.2017.89>.
34. Zabolotny, J.M., Kim, Y.B., Peroni, O.D., Kim, J.K., Pani, M.A., Boss, O., Klamann, L.D., Kamatkar, S., Shulman, G.I., Kahn, B.B., and Neel, B.G. (2001). Overexpression of the LAR (leukocyte antigen-related) protein-tyrosine phosphatase in muscle causes insulin resistance. *Proc. Natl. Acad. Sci. USA* 98, 5187–5192. <https://doi.org/10.1073/pnas.071050398>.
35. Moller, D.E. (2001). New drug targets for type 2 diabetes and the metabolic syndrome. *Nature* 414, 821–827. <https://doi.org/10.1038/414821a>.
36. Elchebly, M., Payette, P., Michaliszyn, E., Cromlish, W., Collins, S., Loy, A.L., Normandin, D., Cheng, A., Himms-Hagen, J., Chan, C.C., et al. (1999). Increased insulin sensitivity and obesity resistance in mice lacking the protein tyrosine phosphatase-1B gene. *Science* 283, 1544–1548. <https://doi.org/10.1126/science.283.5407.1544>.
37. Krebs, D.L., and Hilton, D.J. (2003). A new role for SOCS in insulin action. Suppressor of cytokine signaling. *Sci. STKE* 2003, PE6. <https://doi.org/10.1126/stke.2003.169.pe6>.
38. Emanuelli, B., Peraldi, P., Filloux, C., Sawka-Verhelle, D., Hilton, D., and Van Obberghen, E. (2000). SOCS-3 is an insulin-induced negative regulator of insulin signaling. *J. Biol. Chem.* 275, 15985–15991. <https://doi.org/10.1074/jbc.275.21.15985>.
39. Teimouri, M., Hosseini, H., ArabSadeghabadi, Z., Babaei-Khorzoughi, R., Gorgani-Firuzjaee, S., and Meshkani, R. (2022). The role of protein tyrosine phosphatase 1B (PTP1B) in the pathogenesis of type 2 diabetes mellitus and its complications. *J. Physiol. Biochem.* 78, 307–322. <https://doi.org/10.1007/s13105-021-00860-7>.
40. Xu, E., Schwab, M., and Marette, A. (2014). Role of protein tyrosine phosphatases in the modulation of insulin signaling and their implication in the pathogenesis of obesity-linked insulin resistance. *Rev. Endocr. Metab. Disord.* 15, 79–97. <https://doi.org/10.1007/s11154-013-9282-4>.
41. Hashimoto, N., Feener, E.P., Zhang, W.R., and Goldstein, B.J. (1992). Insulin receptor protein-tyrosine phosphatases. Leukocyte common antigen-related phosphatase rapidly deactivates the insulin receptor kinase by preferential dephosphorylation of the receptor regulatory domain. *J. Biol. Chem.* 267, 13811–13814.
42. Liu, W., Yu, B., Xu, G., Xu, W.R., Loh, M.L., Tang, L.D., and Qu, C.K. (2013). Identification of cryptotanshinone as an inhibitor of oncogenic protein tyrosine phosphatase SHP2 (PTPN11). *J. Med. Chem.* 56, 7212–7221. <https://doi.org/10.1021/jm400474r>.
43. Liang, L.F., Gao, L.X., Li, J., Tagliatalata-Scafati, O., and Guo, Y.W. (2013). Cembrane diterpenoids from the soft coral *Sarcophyton trocheliophorum* Marenzeller as a new class of PTP1B inhibitors. *Bioorg. Med. Chem.* 21, 5076–5080. <https://doi.org/10.1016/j.bmc.2013.06.043>.
44. Zhang, W., Hong, D., Zhou, Y., Zhang, Y., Shen, Q., Li, J.Y., Hu, L.H., and Li, J. (2006). Ursolic acid and its derivative inhibit protein tyrosine phosphatase 1B, enhancing insulin receptor phosphorylation and stimulating glucose uptake. *Biochim. Biophys. Acta* 1760, 1505–1512. <https://doi.org/10.1016/j.bbagen.2006.05.009>.
45. Zhang, S., Liu, S., Tao, R., Wei, D., Chen, L., Shen, W., Yu, Z.H., Wang, L., Jones, D.R., Dong, X.C., and Zhang, Z.Y. (2012). A highly selective and potent PTP-MEG2 inhibitor with therapeutic potential for type 2 diabetes. *J. Am. Chem. Soc.* 134, 18116–18124. <https://doi.org/10.1021/ja308212y>.

STAR★METHODS

KEY RESOURCES TABLE

REAGENT or RESOURCE	SOURCE	IDENTIFIER
Antibodies		
pAKT	Cell Signaling Technology	CAT#4060s RRID: AB_2315049
AKT	Cell Signaling Technology	CAT#9272s; RRID: AB_329827
pIR	Cell Signaling Technology	CAT#3024s; RRID: AB_331253
IR	Cell Signaling Technology	CAT#9750s; RRID: AB_10950969
pIRS	Abcam	CAT#ab66153; RRID: AB_1140753
IRS	Abcam	CAT#ab46800; RRID: AB_881460
PTPRF	Cell Signaling Technology	CAT#17164; RRID: AB_2798778
PTP1B	Cell Signaling Technology	CAT#5311s; RRID: AB_10695100
Beta-actin	Cell Signaling Technology	CAT#4968s; RRID: AB_2313904
Anti-rabbit IgG-HRP antibody	Santa Cruz Biotechnology	CAT#sc-2077; RRID: AB_631745
Anti-mouse IgG-HRP antibody	Santa Cruz Biotechnology	CAT#sc-2314; RRID: AB_641170
SOCS3	Cell Signaling Technology	Cat# 52113, RRID_AB_2799408
Chemicals, peptides, and recombinant proteins		
Insulin	Eli Lilly	N/A
DAPI	Fisher Scientific	CAT#D1306
Fetal bovine serum	Gibco	CAT#10099-141
DMEM	Gibco	CAT#11965-092
Triton X-100	Roche	CAT#11332481001
TRIzol Reagent	Ambion	CAT#10296028
Trizol LS Reagent	Ambion	Cat# 10296
60% high fat diet	Research Diets	CAT#D12492
RIPA buffer (10x)	Cell Signaling Technology	CAT# 9806
LIPOFECTAMINE 2000 REAGENT	Invitrogen	CAT#11668019
Reverse Transcriptase XL (AMV)	Takara	CAT#2621
dNTP Mixture	Takara	CAT#4019
Taq™ PCR	Takara	CAT#R500Z
Critical commercial assays		
ECL Western Blotting Substrate	Thermo Fisher	CAT#32106
Mouse Insulin Elisa kit	Mercodia	CAT#10-1247-01
HDL kit	Nanjing Jiancheng	CAT#A112-1
LDL kit	Nanjing Jiancheng	CAT#A113-1

(Continued on next page)

Continued

REAGENT or RESOURCE	SOURCE	IDENTIFIER
TG kit	Nanjing Jiancheng	CAT#A110-1
TC kit	Nanjing Jiancheng	CAT#A111-1
Plant MicroRNA Kit	Bioteke	CAT#RP5331
BCA Protein Quantification Kit	Vazyme	CAT#E112-02
Universal Plant MicroRNAKit	BioTeke	CAT#RP5377

Deposited data

[GEO]: [GSE248826]	GEO	https://www.ncbi.nlm.nih.gov/geo/query/acc.cgi?acc=GSE248826
[GEO]: [GSE247265]	GEO	https://www.ncbi.nlm.nih.gov/geo/query/acc.cgi?acc=GSE247265
[GEO]:[GSE248220]	GEO	https://www.ncbi.nlm.nih.gov/geo/query/acc.cgi?acc=GSE248220
[Mendeley date]: [https://doi.org/10.17632/756msjkj96.1]	Mendeley date	https://doi.org/10.17632/756msjkj96.1

Experimental models: Cell lines

Hepa 1–6 cell line	ATCC	BFN60700206
HEK293 cell line	ATCC	CRL-11268

Experimental models: Organisms/strains

Mouse: C57BL/6J	NBRI	CAT# N000013
-----------------	------	--------------

Oligonucleotides

Taqman probe miR8175	Thermo Fisher Scientific	CAT#4440887
Taqman probe miR894	Thermo Fisher Scientific	CAT#4440886
Taqman probe miR172a	Thermo Fisher Scientific	CAT#4427975
Taqman probe miR6118-3p	Thermo Fisher Scientific	CAT#4440886
Taqman probe miR6113	Thermo Fisher Scientific	CAT#4440886
Taqman probe miR156	Thermo Fisher Scientific	CAT#4427975
Taqman probe miR168-5p	Thermo Fisher Scientific	CAT#4440887
Taqman probe U6		CAT#4427975
miR8175-primer forward	GenScript	ACACTCCAGCTGGGGATCCCCGGCAACG
miR8175-primer Reverse	GenScript	CTCAACTGGTGTCTGGAGTCGGC AATTCAGTTGAGTGGCGCCG
miR6300-primer forward	GenScript	ACACTCCAGCTGGGGTCTGTGTAGTA
miR6300-primer Reverse	GenScript	CTCAACTGGTGTCTGGAGTCGG CAATTCAGTTGAGCCACTATA
miR8175	GenScript	N/A

Software and algorithms

GraphPad Prism 8	Graphpad	RRID: SCR_002798
Fiji-ImageJ	National Inst. Of Health	RRID: SCR_003070

RESOURCE AVAILABILITY

Lead contact

Further information and requests for reagents and resources should be directed to and will be fulfilled by the lead contacts, Yujing Zhang (yjzhang@nju.edu.cn).

Materials availability

This study did not generate new unique reagents.

Data and code availability

- The RNA-seq data have been deposited in the NCBI Gene Expression Omnibus under accession number GEO: GSE248826, GSE247265, GSE248220. The accession number is listed in the [key resources table](#). “Raw data from [Figures 1, 2, 3, 4, 5, and 6](#) were deposited on Mendeley at [Mendeley: <https://doi.org/10.17632/756msjkj96.1>]
- This paper does not report any original code.
- Any additional information required to reanalyze the data reported in this paper is available from the [lead contact](#) upon request.

EXPERIMENTAL MODEL AND STUDY PARTICIPANT DETAILS

Animal

Male C57BL/6J mice were obtained from the Model Animal Research Center of Nanjing University. Animal experiments were approved by the Animal Research Ethics Committee of Nanjing University and all experiments conformed to the relevant regulatory standards. All animals were C57BL/6J background. Only male mice were used. The experiment used 8-week-old mice, and the experiment ended when they were 24 weeks old. Mice were housed under a 12-h light/dark cycle in individual ventilated cages (IVC) with temperature controlled at 21°C–23°C. Eight-week-old mice were given a high-fat diet containing 60% fat, and *in vivo* experiments were performed after 8 weeks on the high-fat diet. For burdock decoction, mice were gavage fed daily with burdock decoction (500 μ L) or physiological saline for six weeks, and maintained a high-fat diet during the gavage period. For synthetic miR8175, mice were gavage fed daily with synthetic miR8175 (1nmol) or ncRNA for six weeks, and maintained a high-fat diet during the gavage period. To investigate the kinetics of miR8175 in mice, the mice were gavage fed with burdock decoction (500 μ L) or 1 nmol synthetic miR8175, at different time intervals (1, 3, 6 or 12 h), mice were sacrificed to collect the plasma samples and tissue samples for extracting total RNA.

Cell

Hepa1-6 cells were purchased from the China Cell Culture Center (Shanghai, China). The cells were cultured using DMEM (Gibco) with 10% FBS (Gibco). The cell was routinely tested and confirmed to be free of mycoplasma (YK-DP-20, Ubigen Biosciences, Guangzhou, China). Synthetic miR8175 or ncRNA was transfected into hepa1-6 using Lipofectamine2000 (Invitrogen). After a 24-h incubation period, the cells were washed with PBS and then lysed using RIPA buffer.

METHOD DETAILS

Burdock decoction

We obtained burdock root from a traditional Chinese herbal medicine store. The burdock roots (60 g) were immersed in 700 mL of water for a duration of 30 min, and then boiled for 30 min, resulting in ~80 mL of decoction.

RNA extraction

RNA extraction from burdock decoction

First, we extracted the RNA from the burdock decoction using the phenol-chloroform method. Then, small RNAs in precipitated RNA were extracted using a Universal Plant MicroRNA Kit (Biotek) following the manufacturer’s instructions.

RNA extraction from burdock root

First, add 100mg of tissue to 1mL of extraction buffer (5 mM EDTA, 0.2 M Tris-HCl, 0.2 M LiCl, 1/1000 volume of β -mercaptoethanol). After grinding, the supernatant was transferred, and an equal volume of TRIzol LS (Ambion) was added. Then, small RNAs in precipitated RNA were extracted using a Universal Plant MicroRNA Kit.

RNA extraction from serum and tissues

Total RNA in serum and isolated tissue were extracted by phenol-chloroform method and TRIzol reagent (Ambion), respectively.

qRT-PCR of plant microRNA

We performed qRT-PCR using TaqMan miRNA probes (Applied Thermo Fisher). In tissues, plant-miRNA expression levels were normalized to U6 expression (Applied Thermo Fisher). We estimated relative miRNA expression levels using $2^{-\Delta\Delta Ct}$ (ΔCt sample– ΔCt control). For serum, burdock decoction, and burdock, the absolute expression level of miRNA was calculated using the corresponding standard curve. We reverse transcribed a series of miRNAs at known concentrations using synthetic miRNA oligonucleotides. qRT-PCR was performed using a LightCycler 480 II (Roche).

Illumina deep sequencing

RNAs from burdock decoction were isolated following the method described above. Illumina sequencing was performed by BGI (Shenzhen, China).

Pull-down experiment

The biotin-modified miR8175 mimics were transfected into Hepa1-6 cells, and total RNA was collected 24 h after transfection. The RNA bound to miR8175 was enriched using streptavidin-coated magnetic beads and analyzed by deep sequencing. To prepare the sequencing library, the Illumina TruSeq RNA Sample Prep Kit (Cat#FC-122-1001) was utilized. RNA sequencing was performed on the Illumina HiSeq 2500 platform, and the analysis was conducted by CapitalBio Technology (Beijing, China).

RNA-seq library preparation and sequencing

The total RNA extraction used for sequencing was evaluated using TRIzol reagents (Invitrogen, Pleasanton, CA, USA) and the quantity and purity of the obtained total RNA were evaluated using Bioanalyzer 2100 (Agilent, Santa Clara, CA, USA). RNA sequencing libraries were generated using the Illumina TruSeq RNA Sample Prep Kit (Cat#FC-122-1001), starting with approximately 1 µg of total RNA. Single-end sequencing was conducted on an Illumina HiSeq 2500 platform at Capitalbio (Beijing, China).

Western blot

Add protease and phosphatase inhibitor (Sangon) to RIPA buffer (CST) to prepare lysis solution for cell or tissue lysis, the supernatant was retained for Western blot analysis. The samples were subjected to 10% or 8% SDS polyacrylamide gel electrophoresis, and then transferred onto a PVDF membrane (Roche). Subsequently, incubate the membrane with the first antibody at room temperature for 3 h or at 4°C overnight. The primary antibodies included phosphor-Akt (Ser473, CST), Akt (CST), GAPDH (Santa Cruz) and β-actin (CST). The secondary antibodies included goat antirabbit (CST) and goat antimouse (CST). The bands were detected using an imaging system (Tannon).

Glucose tolerance test and insulin tolerance test

After fasting overnight, mice underwent glucose tolerance tests, and then intraperitoneal injected with 1 g/kg weight glucose, blood glucose levels were detected after 15, 30, 60 and 90 min via the tail vein. After fasting 6 h, mice were intraperitoneal injected with insulin (0.75 units/kg body weight) and were detected blood glucose levels after 15, 30, 60, 90 and 120 min via the tail vein.

Evaluate insulin sensitivity in mouse liver

Mice were fasted for 6 h and injected with 0.75 units/kg of insulin. After 15 min, the mice were euthanized, and liver tissues were collected. The expression levels of pAKT in mouse liver before and after insulin stimulation were detected by Western blot.

Histopathological examination of pancreatic tissue

The obtained pancreatic tissue was fixed in 4% paraformaldehyde and embedded in paraffin. Sections of 5 µm in thickness were prepared, and after deparaffinization, the sections were dehydrated with a series of ethanol gradients (100%, 95%, 80%, and 70%). Subsequently, staining was performed using hematoxylin and eosin (H&E), and the size and quantity of islets were analyzed.

sEV isolation

sEV were isolated from mouse serum by differential centrifugation. Briefly, by centrifugation at 300× g to remove cells, at 3000× g to remove other debris, at 10000× g to remove large vesicle. The supernatant was centrifuged by using a high-speed centrifuge to separate extracellular vesicles at 120000× g for 2–3 h.

Plasmid conduction and luciferase assay

Apply TargetScan online software to predict miR8175 target genes. For the luciferase reporter assays, In the luciferase reporter gene detection, the 3'UTR regions of *Ptprf* and *Ptp1b* are inserted downstream of the Renilla luciferase gene, containing potential wild-type or mutant miR8175 binding sites. The HEK293 cells were plated on plate (12-well) and cotransfected with firefly luciferase reporter plasmid (0.4 µg), β-galactosidase expression vector (0.4 µg, Ambion) and equal amountsof mature miR8175 (50 pmol) or ncRNA. After cotransfection for 24 h, the cells were analyzed and the luciferase activity of the Renilla luciferase were detected.

QUANTIFICATION AND STATISTICAL ANALYSIS

We performed our statistical analysis using GraphPad Prism 8.0. The data are presented as the mean ± SE. If it conforms to a normal distribution, perform unpaired Student's t test (double tailed), one-way ANOVA, or two-way ANOVA. If it does not follow a normal distribution, Kruskal Wallis one-way ANOVA will be performed, followed by Dunn multiple comparison test or Mann Whitney U test (double tailed). The level of statistical significance was set at $p < 0.05$.